

Nanocrystallization of the Amorphous $\text{Fe}_{14}\text{Ni}_{40}\text{Zr}_7\text{B}_{12}$ Alloys Studied by the Mössbauer Spectroscopy

M. KOPCEWICZ^{a,*}, B. IDZIKOWSKI^{b,†} AND J. KALINOWSKA^a

^aInstitute of Electronic Materials Technology
Wólczyńska 133, 01-919 Warszawa, Poland

^bInstitute of Molecular Physics, Polish Academy of Sciences
Smoluchowskiego 17, 60-179 Poznań, Poland

Formation of the soft magnetic nanostructure in amorphous $\text{Fe}_{41}\text{Ni}_{40}\text{Zr}_7\text{B}_{12}$ alloy due to heat treatment is studied by the Mössbauer, differential scanning calorimetry, and X-ray diffraction techniques. Annealing at temperatures 520–580°C leads to the formation of extremely soft nanocrystalline alloy as revealed by the rf-Mössbauer measurements. The superparamagnetic behaviour was observed for the alloy annealed at 620–640°C. At higher annealing temperatures good soft magnetic properties deteriorate.

PACS numbers: 76.80.+y, 75.50.Kj, 75.50.Bb, 81.40.-z

1. Introduction

Soft magnetic nanocrystalline alloys, obtained after subsequent annealing of a suitable amorphous precursor, consist of nanocrystalline grains embedded in a residual amorphous matrix [1, 2]. Such nanostructures reveal excellent soft magnetic properties, usually explained in terms of the random anisotropy model [3], related to the suppression of the local magnetocrystalline anisotropy by exchange interaction, combined with high saturation magnetization and high permeability which make them ideally suited for applications in magnetic devices for electronics. Since the discovery of FINEMET alloys [1] and development of ternary Fe–M–B(Cu) NANOPERM alloys [2] the search continues for new nanocrystalline alloys with improved magnetic and mechanical properties.

*corresponding author; e-mail: kopcew_m@sp.itme.edu.pl

†e-mail: idzi@ifmpan.poznan.pl

We prepared the amorphous $\text{Fe}_{81-x}\text{Ni}_x\text{Zr}_7\text{B}_{12}$ ($x = 10 \div 40$) alloys in which the nanostructure was formed by annealing. Structural changes induced by thermal treatment were characterised by the Mössbauer spectroscopy and supplemented by the differential scanning calorimetry (DSC) and X-ray diffraction (XRD) measurements. Magnetic properties of nanocrystalline alloys were studied by the specialised rf-Mössbauer technique [4–6] in which the rf collapse and sidebands effects, induced by the external radio-frequency (rf) magnetic field, are employed [7].

Although all alloys with $x = 10 \div 40$ were studied our discussion is focused on the $\text{Fe}_{41}\text{Ni}_{40}\text{Zr}_7\text{B}_{12}$ alloy because it reveals most interesting magnetic properties.

2. Experimental details

Amorphous $\text{Fe}_{81-x}\text{Ni}_x\text{Zr}_7\text{B}_{12}$ ($x = 10 \div 40$) ribbons (3–4 mm wide and 20–25 μm thick) were prepared by rapid quenching from the melt. Amorphous $\text{Fe}_{41}\text{Ni}_{40}\text{Zr}_7\text{B}_{12}$ precursor was annealed in vacuum for 1 hour at $T_A = 440\text{--}800^\circ\text{C}$. Conventional Mössbauer measurements were performed at room temperature for all as-quenched and annealed samples. For sample annealed at $620\text{--}640^\circ\text{C}$ the Mössbauer measurements were performed also at low temperatures (295–80 K). The rf-Mössbauer measurements were carried out during exposure of the sample to the 61 MHz rf field of intensity ranging from 0 to 20 Oe in the same way as in our earlier studies [4–7].

3. Results and discussion

Amorphous $\text{Fe}_{41}\text{Ni}_{40}\text{Zr}_7\text{B}_{12}$ alloy crystallises in two steps, as shown in the DSC measurements. The crystallization temperatures of the first and second crystallization step are about 480°C and 650°C . The Mössbauer spectra recorded for the $\text{Fe}_{41}\text{Ni}_{40}\text{Zr}_7\text{B}_{12}$ alloy annealed at indicated temperatures are shown in Fig. 1. The XRD and Mössbauer measurements have shown that all as-quenched alloys are fully amorphous (Fig. 1a). As can be seen, the crystalline bcc-Fe phase forms in the sample annealed at 470°C , in addition to the residual amorphous phase (Fig. 1b). An increase in annealing temperature causes an increase in the spectral contribution of the bcc-Fe phase (Fig. 1c). Then at $T_A \geq 570^\circ\text{C}$ the spectral contribution of this component decreases which is associated with the simultaneous change of the spectral component related to the broadened sextet which now corresponds both to the residual amorphous phase and to the Ni-containing nanostructure (Fig. 1d). The H_{hf} of this sextet slightly decreases which suggests a substantial Ni content in the nanocrystalline phase (Fig. 1c–e). The XRD measurements performed for these samples suggest that the nanograins of the $(\text{FeNi})_{23}\text{B}_6$ phase are formed at $T_A \approx 570^\circ\text{C}$. At $T_A \approx 595^\circ\text{C}$ the single line component appears in the spectrum (Fig. 1f) and the H_{hf} of the magnetic component further decreases. The single-line component dominates in the spectra recorded for $T_A = 620\text{--}640^\circ\text{C}$ (Fig. 1g, h).

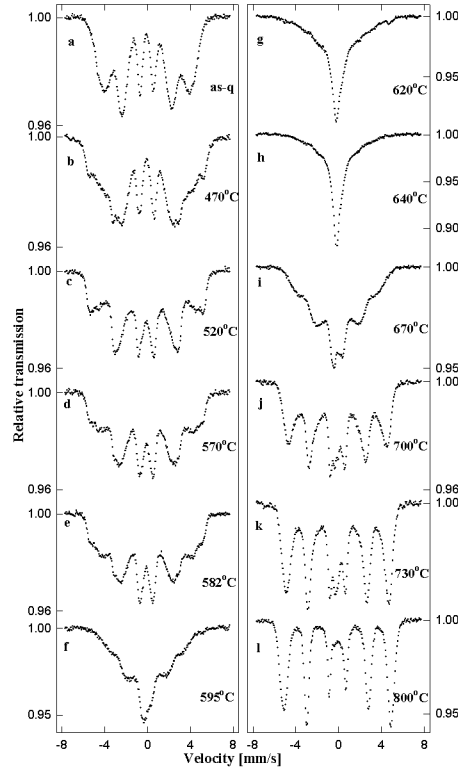


Fig. 1. Room temperature Mössbauer spectra of $\text{Fe}_{41}\text{Ni}_{40}\text{Zr}_7\text{B}_{12}$ alloy annealed at indicated temperatures.

The XRD patterns are almost the same for samples annealed in the temperature range of 570–640°C, whereas the Mössbauer spectra are distinctly different (Figs. 1d and g, h). In order to elucidate the origin of a single line component observed in Fig. 1g the low temperature Mössbauer measurements were performed (Fig. 2). As can be seen from Fig. 2, the spectral fraction of a single line strongly decreases with decreasing temperature and the magnetic component increases. The single line transforms gradually to the magnetic pattern (Fig. 3) which rules out a simple para- to ferromagnetic phase transition. The observed gradual transformation of the single line to a magnetic pattern may suggest a superparamagnetic relaxation origin of this line. Very similar behaviour was observed for the sample annealed at 640°C. Most probably at favourable temperatures (620–640°C) the crystalline phase of the FeNi-type is formed as very small nanograins separated by a residual amorphous matrix, probably of iron poor NiZrB-type that may allow a superparamagnetic relaxation. However, the presence of such an intergranular phase would be difficult to detect by the Mössbauer and XRD techniques. Su-

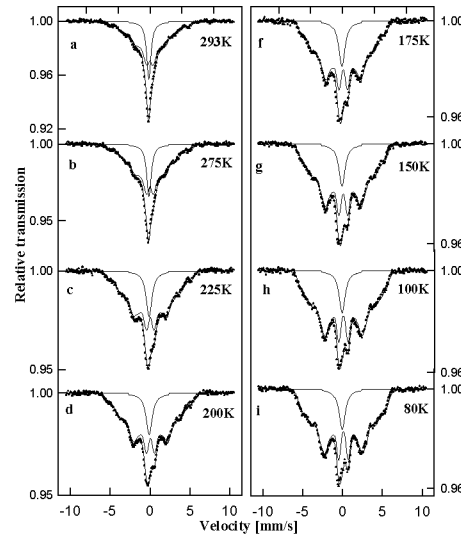


Fig. 2. Low temperature Mössbauer spectra of $\text{Fe}_{41}\text{Ni}_{40}\text{Zr}_7\text{B}_{12}$ alloy ($T_A = 620^\circ\text{C}$).

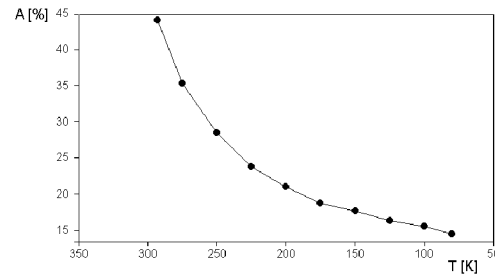


Fig. 3. Temperature dependence of a single line component in the spectra shown in Fig. 2.

perparamagnetic behaviour in nanocrystalline alloys when residual nonmagnetic amorphous matrix separates the nanograins was suggested recently [8–10].

At higher annealing temperatures no relaxation behaviour was observed because grains grow and microcrystalline magnetic phases are formed (Fig. 1j–l).

Conversion electron Mössbauer spectra (CEMS), which provide information regarding a near surface region of the sample, about 120 nm thick, do not show a single line component. This suggests that in the surface regions of the samples the superparamagnetic relaxation is suppressed, probably by the additional anisotropy related to the stress induced by the enhanced surface crystallization.

The increase in T_A above the temperature of the second crystallization peak in DSC curve causes a complete crystallization of the sample and the single-line component disappears (Fig. 1j–l). The phase formed at $T_A \geq 700^\circ\text{C}$ (Fig. 1j–l) is most probably fcc-FeNi.

The soft magnetic properties of $\text{Fe}_{41}\text{Ni}_{40}\text{Zr}_7\text{B}_{12}$ nanocrystalline alloy were verified by the rf-Mössbauer technique [4–7]. The Mössbauer spectra recorded during the exposure of the $\text{Fe}_{41}\text{Ni}_{40}\text{Zr}_7\text{B}_{12}$ as-quenched and annealed at 520°C and 582°C alloys to the rf field of 61 MHz at various rf field intensities are shown in Fig. 4. A gradual rf-induced narrowing of the magnetic hyperfine structure (mhfs) is observed for the amorphous alloy (Fig. 4a–f). A complete rf collapse of the mhfs to a quadrupole doublet is observed for the rf field of 12 Oe (Fig. 4e). However, at 6 Oe the rf-induced narrowing is only marginal (Fig. 4c). This means that the effective anisotropy field in the amorphous state is considerably larger than 6 Oe but smaller than 12 Oe. The formation of the nanocrystalline phase at $T_A = 520^\circ\text{C}$ causes changes of the rf-Mössbauer spectra (Fig. 4b'–f'). The spectra are significantly more collapsed as compared with the amorphous alloy (Fig. 4c, d). Substantial rf-induced narrowing of the mhfs occurs already at 6 Oe (Fig. 4c') and at 8 Oe the rf-collapsed central component accompanied by a partly collapsed magnetic “wings” appears (Fig. 4d'). The shape of the spectra in Figs. 4c' and 4d' suggest a two-phase structure consisting of magnetically very soft nanocrystalline grains, which produce a collapsed central part of the spectra, and the amorphous matrix with a larger anisotropy related to the partly collapsed

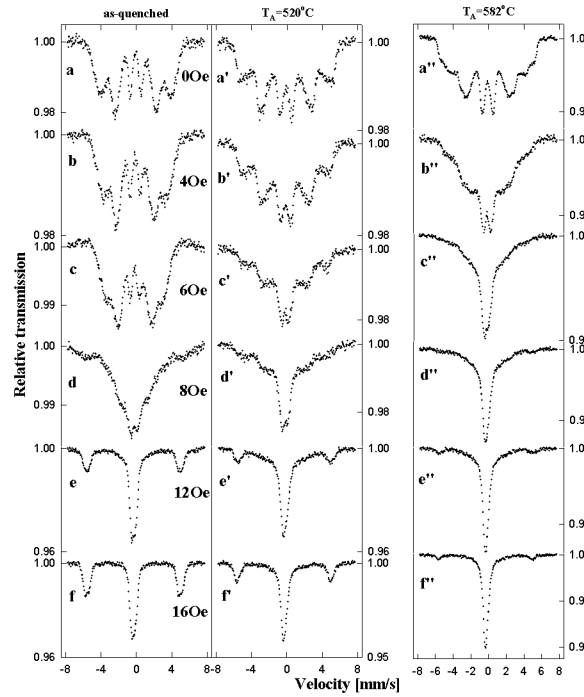


Fig. 4. The rf-Mössbauer spectra of $\text{Fe}_{41}\text{Ni}_{40}\text{Zr}_7\text{B}_{12}$ alloy: as-quenched (a–f), annealed at 520°C (a'–f'), annealed at 582°C (a''–f'').

magnetic component. A further increase in rf field intensity leads to an almost complete collapse of the mhfs of the magnetic component. The central collapsed single line and rf sidebands appear in the spectrum (Fig. 4e'). Such an rf field is sufficiently strong to average the hyperfine fields both in the residual amorphous matrix and nanocrystalline bcc-grains. However, the magnetostriction of the alloy is still substantial, as shown by fairly strong rf sidebands (Fig. 4f'). The most interesting results were obtained for the $\text{Fe}_{41}\text{Ni}_{40}\text{Zr}_7\text{B}_{12}$ alloy annealed at 582°C (Figs. 4a''–f''). The rf-Mössbauer spectrum reveals a substantial collapse for the rf field intensity of only 4 Oe (Fig. 4b'') at which the amorphous alloy did not show any narrowing of mhfs (Fig. 4b). At 6 Oe the mhfs strongly narrows (Fig. 4c'') and 8 Oe rf field is sufficient for an almost complete collapse of the mhfs to a single line associated with the bcc grains, accompanied by small magnetic “wings”, most probably related to a still incomplete collapse of the mhfs of the residual amorphous phase. A 12 Oe rf field induces a complete collapse of mhfs of the entire nanocrystalline alloy and weak sidebands appear in the spectrum (Fig. 4e''). Such an rf field dependence of the rf-Mössbauer spectra reveals that the effective anisotropy of the alloy annealed at 582°C is particularly small, considerably smaller than in the amorphous alloy and in the sample annealed at lower temperatures. Till now in all rf-Mössbauer studies performed for various NANOPERM alloys (e.g., [4, 5, 6, 11]) the amorphous precursor and residual amorphous matrix had a smaller anisotropy than the nanocrystalline bcc-Fe grains. In the present case of $\text{Fe}_{41}\text{Ni}_{40}\text{Zr}_7\text{B}_{12}$ alloy annealed at the optimal temperature the crystalline Ni-containing nanostructure reveals substantially a smaller anisotropy than the residual amorphous matrix and the amorphous precursor.

Striking differences as regards the rf sidebands effect, directly related to the magnetostriction [12], could be noticed in the rf-Mössbauer spectra recorded for 16 Oe rf field (Figs. 4f, f', and f''). Whereas the rf collapse is complete for all alloys in Fig. 4, the rf sideband intensities strongly decrease in the nanocrystalline alloys and are the smallest for the alloy annealed at 582°C . Thus the alloy annealed at 582°C has the best soft magnetic properties: the smallest anisotropy and almost vanishing magnetostriction.

Annealing the $\text{Fe}_{41}\text{Ni}_{40}\text{Zr}_7\text{B}_{12}$ alloy at temperatures exceeding the second crystallization step ($T_A \geq 730^\circ\text{C}$) leads to the formation of the phase which is magnetically much harder. The rf-Mössbauer spectra recorded for samples annealed at 730°C and 800°C reveal only marginal rf-induced narrowing of the magnetically split broad sextets.

Despite the fact that the hyperfine field in the $\text{Fe}_{41}\text{Ni}_{40}\text{Zr}_7\text{B}_{12}$ nanocrystalline alloy is reduced as compared with the bcc-Fe phase in NANOPERM alloys, an improved magnetic softness combined with the much reduced brittleness of the samples offer new attractive possibilities for technical applications of these novel Ni-containing alloys.

Acknowledgments

Financial supports from the grant No. KBN 2 P03B 06815 from the State Committee for Scientific Research and from NEDO (Japan) "Nanopatterned magnets" project are gratefully acknowledged.

References

- [1] Y. Yoshizawa, S. Oguma, K. Yamauchi, *J. Appl. Phys.* **64**, 6044 (1988).
- [2] K. Suzuki, A. Makino, A. Inoue, T. Masumoto, *J. Appl. Phys.* **74**, 3316 (1993).
- [3] G. Herzer, *Mater. Sci. Eng. A* **133**, 1 (1991).
- [4] M. Kopcewicz, A. Grabias, P. Nowicki, D.L. Williamson, *J. Appl. Phys.* **79**, 993 (1996).
- [5] M. Kopcewicz, A. Grabias, D.L. Williamson, *J. Appl. Phys.* **82**, 1747 (1997).
- [6] M. Kopcewicz, *Acta Phys. Pol. A* **96**, 49 (1999).
- [7] M. Kopcewicz, *Struct. Chem.* **2**, 313 (1991).
- [8] I. Škorvánek, R.C. O'Handley, *J. Magn. Magn. Mater.* **140-144**, 467 (1995).
- [9] N. Randrianantoandro, A. Ślawska-Waniewska, J.M. Greneche, *Phys. Rev. B* **56**, 10797 (1997).
- [10] T. Kemény, D. Kaptás, J. Balogh, L.F. Kiss, T. Pustai, I. Vincze, *J. Phys., Condens. Matter.* **11**, 2841 (1999).
- [11] M. Kopcewicz, A. Grabias, B. Idzikowski, *Mater. Res. Soc. Symp. Proc.* **577**, 487 (1999).
- [12] L. Pfeiffer, N.D. Heiman, J.C. Walker, *Phys. Rev. B* **6**, 74 (1972).